

Si-Micromachined Coplanar Waveguides for Use in High-Frequency Circuits

Katherine Juliet Herrick, Thomas A. Schwarz, and Linda P. B. Katehi, *Fellow, IEEE*

Abstract—This paper describes the development and characterization of a new class of Si-micromachined lines and circuit components for operation between 2–110 GHz. In these lines, which are a finite-ground coplanar-waveguide (FGC) type, Si micromachining is used to remove the dielectric material from the aperture regions in an effort to reduce dispersion and minimize propagation loss. Measured results have shown a considerable loss reduction to levels that compare favorably with those of membrane lines and rectangular waveguides. Micromachined FGC lines have been used to develop *V*- and *W*-band bandpass filters. The *W*-band micromachined FGC filter has shown a 0.8-dB improvement in insertion loss at 94 GHz over a conventional FGC line. This approach offers an excellent alternative to the membrane technology, exhibiting very low loss, no dispersion, and mode-free operation without using membranes to support the interconnect structure.

Index Terms—Coplanar waveguide, micromachining.

I. INTRODUCTION

DESPITE the success achieved in most monolithic microwave integrated circuit (MMIC) implementations, high power has remained a challenge. The low output power of solid-state sources, along with their low impedance, is further hindered by conventional transmission-line characteristics, resulting in very low efficiencies. From a device performance point of view, it is clear that traditional planar-line techniques introduce high losses due to the excitation of substrate-wave modes. While parasitic radiation is inherent to microstrip, attempts to suppress it with ground connections can be achieved using via-hole technology. Via holes, however, result in high parasitic inductance and radiation leading to substantial device-gain degradation with a detrimental impact on circuit operation at millimeter-wave frequencies. Conventional coplanar technology provides limited solutions to some of these problems by bringing the ground plane to the proximity of the active devices at the cost of additional parasitic effects, such as the excitation of parallel plate and microstrip modes. These effects require geometry modifications and transmission media, such as channelized waveguides, which are difficult to implement, especially at higher frequencies.

As shown recently [1], [2], the finite ground coplanar (FGC) lines, shown in Fig. 1(a), provide an excellent alternative to conventional microstrip or coplanar waveguide

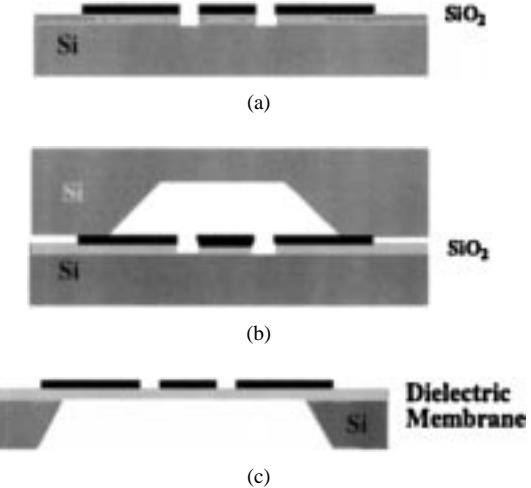


Fig. 1. (a) FGC on high-resistivity Si. (b) Packaged FGC. (c) Membrane FGC (microshield).

(CPW) for millimeter- and submillimeter-wave applications. This line is printed on high-resistivity Si with a thin layer of thermally grown SiO₂. After metal deposition, the oxide is removed from the line apertures to avoid dielectric losses from post-processing oxide contaminants. These lines have exhibited very low-loss characteristics [26] and the capability to operate on a variety of substrates with or without back-side metallization and without vias for ground equalization. These characteristics have made them exceptional candidates for high-frequency low-cost high-performance circuits. Furthermore, mode-free TEM operation allows for quasi-static modeling, as already demonstrated by the excellent agreement between measured data and LIBRA's quasi-static analysis for frequencies up to 110 GHz [27]–[29]. The exhibited low loss is responsible for the excellent performance exhibited by a variety of stubs and filters, designed for operation at *W*-band [26], [27]. Additionally, the use of FGC lines in *W*-band detectors has demonstrated bandwidths in excess of 30% with sensitivities as high as 3100 V/W. Furthermore, multiplier circuits based on this type of line have demonstrated very high power levels at frequencies exceeding 77 GHz [28], [29].

The study of FGC lines has demonstrated that line loss is predominantly due to ohmic loss in the metallic conductors. This is not to say that the excited field is unaffected by the dielectric material. In fact, the material itself influences the propagation characteristics by increasing the value of the effective dielectric constant from 1, for an air-suspended

Manuscript received November 11, 1997; revised March 4, 1998. This work was supported by the Office of Naval Research under Grant N00014-95-1-1299 and by Hughes under the DARPA Program FR-573420-SR8.

The authors are with the University of Michigan, Ann Arbor, MI 48109 USA.

Publisher Item Identifier S 0018-9480(98)04038-1.

coplanar line such as the membrane FGC shown in Fig. 1(c), to approximately 6, for the FGC printed on a high-resistivity silicon wafer [see Fig. 1(a) and (b)]. In a line where ohmic losses are primarily responsible for loss performance, the only other parameter that can further influence loss is the characteristic impedance. By increasing the characteristic impedance of the line, the current distribution on the conductors decreases, thus leading to reduced loss per guided wavelength.

It is known that the characteristic impedance of FGC lines strongly depends on its geometrical parameters including the center conductor width, ground width, and conductor separation. An increase of the characteristic impedance to values above 75Ω requires either a narrow signal conductor leading to current crowding, or wider aperture dimensions, leading to multimoding. To increase the line impedance without encountering the above problems, material can be removed with appropriate chemical processes. As previously reported in the literature, substrate material under the line can be removed by wet etching and the line can be suspended in air by Si bars periodically placed along the metallic structure [2]. This approach is limited by fabrication complexity which becomes prohibitive with increasing circuit density. In another effort, the material of the host wafer is removed in a similar way and the interconnect structure is supported by a thin dielectric membrane grown on the surface of the substrate [1], [2]–[5], [14], [18]. While the use of membranes has demonstrated the lowest loss by a planar interconnect, they are limited by the need for backside processing, complexity of the layout, and size of the required membrane. Herein, we present another approach which effectively removes material underneath the line without requiring suspension of the center conductor in free space. In the following sections, an extensive discussion of the propagation characteristics of micromachined FGC lines will demonstrate the potential of this new class of interconnects. The presented study will conclude with a description of *V*- and *W*-band micromachined FGC filters and a comparison of their electrical performance with that of conventional CPW filters operating in the same frequency range.

II. MICROMACHINED CPW

During the past five years, our group at the University of Michigan has undertaken an extensive effort toward the development of high-frequency micromachining technology [1]–[12], [14], [18]. This technology is based on a simple idea: to introduce, through established MMIC processes, structural changes in the semiconducting wafers (Si, GaAs, or InP, etc.) to improve circuit performance, attain additional functionality, and introduce new integration capabilities. This approach has shown tremendous potential in transforming existing MMIC's into a new generation of devices and circuits which are characterized by a substantial increase in generated power capability and considerable cost benefits [14].

Herein, the implementation of this concept in FGC circuits operating in *Ka*-, *V*-, and *W*-bands is demonstrated to provide excellent loss reduction. In coplanar lines, the field is tightly concentrated in the apertures between the conductors. When material in this area is removed, the line capacitance is reduced and leads to less current flowing in the conductors. As a result,

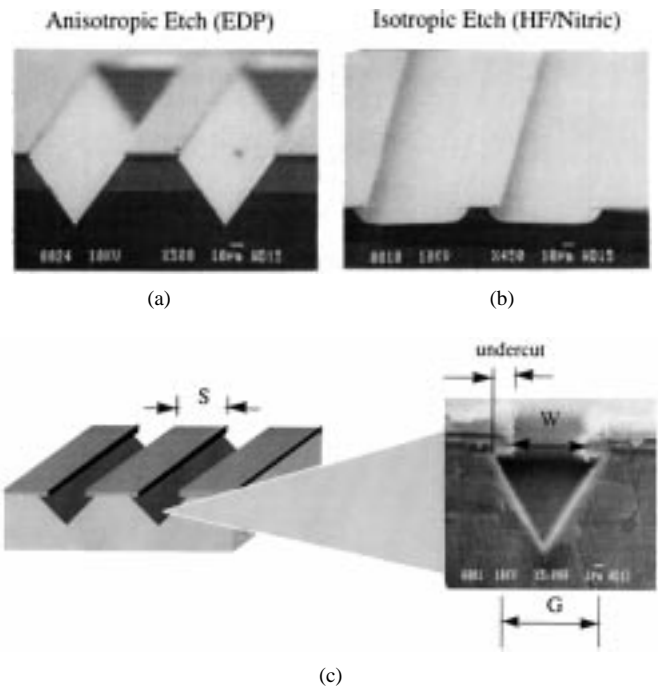


Fig. 2. High-performance micromachined FGC. (a) Etched by EDP. (b) Etched by HF/Nitric. (c) Cross section of the line.

the line exhibits lower loss and lower parasitic capacitances while it reduces reflections at junctions. Fig. 2 shows micromachined CPW's where material has been removed from the aperture regions by wet etching using ethylenediamine pyrocatechol (EDP) [see Fig. 2(a)] and hydrofluoric/nitric acid solution (HF/Nitric) [see Fig. 2(b)]. The resulting line exhibits lower ohmic, dielectric, and radiation loss in addition to lower parasitics. These micromachined lines can be fabricated on full thickness substrates with no wafer thinning or via holes for ground equalization. The line characteristics are independent of wafer thickness, so several wafers can be stacked to form a three-dimensional structure with no effect on the line characteristics. The lines propagate a near-TEM mode with very little dispersion. The effective dielectric constant of the micromachined FGC lines is constant within $\pm 1\%$ from 4 to 110 GHz, while junction parasitics are very weak. These properties simplify the design of millimeter-wave components and provide excellent electrical performance. The design, fabrication, and measurement of interconnects and filters based on this micromachined line technology will be discussed in detail below.

A. Design of Micromachined Lines

Micromachined FGC lines (see Fig. 2) have a geometry similar to conventional FGC lines, except that the material underneath the line apertures has been removed, as previously discussed. The shape of the groove created by the etchant strongly depends on the solution and the time of the etch. The resulting micromachined CPW has all the advantages of conventional CPW, including balanced propagation, coplanar configuration, and the capability of front-side wafer processing. The width of the line and the depth of the grooves provide direct control over the cutoff frequency of the next higher

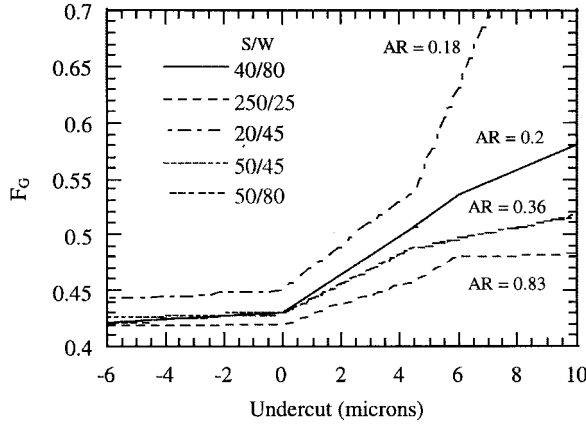


Fig. 3. F_G versus undercut (microns) for five different aspect ratios, S/W where S is the center conductor width and W is the aperture width.

order mode and the range of single-mode propagation. In this paper, our study will focus on EDP-etched FGC's because of the ease in fabrication and control over undercut. The groove size (G) can be defined as the aperture width (W) plus the lateral undercut (U). By appropriately choosing the ground-strip width (W_g), the signal-strip width (S), and groove size (G), the cutoff frequency can be pushed beyond the highest operating frequency. The result is the elimination of parasitic parallel plate/microstrip modes and the reduction of undesired loss. The design equation for this line is given below:

$$2(W_g + W) + S < F_G \lambda_{o, h/2}$$

where $F_G = 1/(\sqrt{\epsilon_{\text{eff}}})$, is directly dependent on the amount of removed material. The electrical parameter F_G is very important to know in order to design lines that operate in the single-mode regime. However, as will be discussed later, F_G is inversely related to the effective dielectric constant and, as a result, strongly depends on the aspect ratio $AR = S/(S+2W)$ and dielectric constant ϵ_r of the substrate. Measurements performed on a variety of lines and for a variety of undercuts U reveal that in a micromachined FGC, the coefficient F_G exhibits a strong dependence on the center conductor width (S) and undercut (U), and is shown to be less critically dependent on the aperture (W). A plot of F_G versus undercut for five different aspect ratios is shown in Fig. 3. Note that for each aperture width, the depth of the center of the V-shaped groove is dictated by the 53.7° angle of the $\langle 111 \rangle$ Si crystal planes. Therefore, the $25\text{-}\mu\text{m}$ aperture yields a center depth of $17\text{ }\mu\text{m}$, whereas that of the $80\text{-}\mu\text{m}$ aperture is $56\text{ }\mu\text{m}$. In the limit of total dielectric removal, F_G goes to 1. As seen in Fig. 3, the two parameters which mostly control F_G are the aspect ratio AR of the line and the undercut U . This indicates that the electric field between the line conductors confines mostly in the aperture region and very little field is penetrating into the substrate. Due to the capability of the line to effectively confine the fields on one side of the wafer, wafer thickness and backside metallization are not critical to performance. As a result, wafer thinning is not required unless is dictated by other circuit layout and size restrictions.

Several micromachined FGC lines and filter circuits have been fabricated on $500\text{-}\mu\text{m}$ -thick Si substrates. The total width

of the line, $2(W_g + W) + S$, has been chosen for all designs to push the cutoff frequency of the first higher order mode to 120 GHz . The backside of the wafer is not metallized, but is in contact with a metal chuck during measurements. Since the realized geometries are symmetric, air-bridges for ground equalization are not included in the circuit.

B. Fabrication

All the micromachined FGC lines studied herein have been fabricated on $500\text{-}\mu\text{m}$ -thick Si substrates with a $1.5\text{-}\mu\text{m}$ $\text{SiO}_2/\text{Si}_3\text{N}_4/\text{SiO}_2$ protective layer. Circuit metallization is obtained via electro-plating $1.7\text{--}2\text{ }\mu\text{m}$ of Cr/Au using liftoff techniques. Si apertures are opened and are anisotropically etched using EDP. Although both isotropic and anisotropic etchants have been investigated [34], anisotropic etching with EDP has been the most reliable. Since this selective etchant stops along the $\langle 111 \rangle$ crystal planes, this method of micromachining is relatively easy to control. Undercut at a rate of $2\text{--}3\text{ }\mu\text{m}/\text{h}$ has been characterized and proven quite repeatable. In the following, lines with $2\text{--}12\text{-}\mu\text{m}$ undercut have been designed, fabricated, and measured to understand the trends of line performance versus undercut for various aspect ratios.

C. Measurements

Following fabrication, S -parameters are measured using a through-reflect-line (TRL) calibration. On-wafer calibration standards consisting of micromachined FGC lines are used with NIST MultiCal software [33]. All measurements are made on an Alessi probe station using pico probes from 2 to 110 GHz , with a gap from 60 to 75 GHz , and several test sets for calibration to cover the desired frequency range. The resulting S -parameter data from the through and delay lines are then processed using MultiCal to compute the propagation constant β and attenuation constant α .

III. MICROMACHINED FGC LINES

Lines of various aspect ratios and groove sizes have been fabricated, and their loss and effective dielectric constant have been measured for frequencies varying from 2 to 110 GHz . Measured results show that the loss and ϵ_{eff} strongly depend on the aspect ratio of the line and on the amount of material removed. As seen from the measurements, ϵ_{eff} is independent to the operating frequency indicating that the line has almost zero dispersion. Specifically, Fig. 4 shows measured values of the effective dielectric constant as a function of frequency, with $W-S-W$ equal to $80\text{--}40\text{--}80\text{ }\mu\text{m}$, for the conventional FGC and micromachined FGC lines with 4- and $12\text{-}\mu\text{m}$ undercut. These are compared to a membrane CPW (microshield) with the same aspect ratio. These results confirm that the removal of the material results in reduction of the effective dielectric constant from the initial value of 5.6 to the final value of 2.72 due to considerable reduction of the line capacitance.

To confirm the measurements, a full-wave finite-element method was used to plot the electric-field distribution in micromachined FGC lines with $8\text{-}\mu\text{m}$ undercut [see Fig. 5(a)] and compared to the field distribution in nonmicromachined FGC lines [see Fig. 5(b)]. From 5(a) and (b), it is clear that

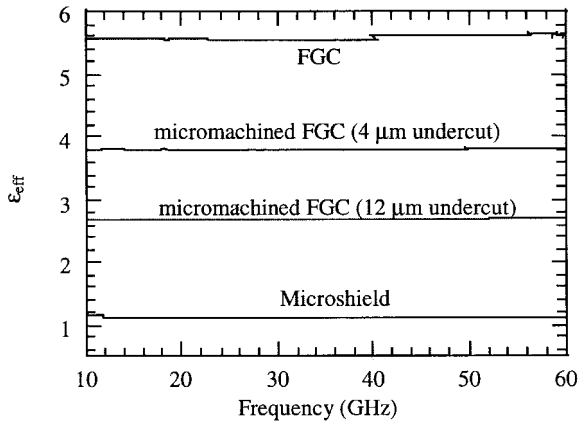
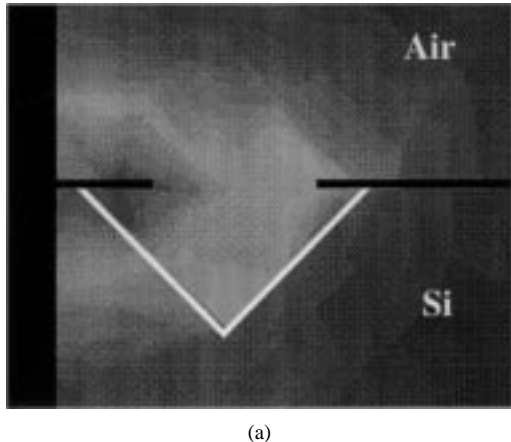
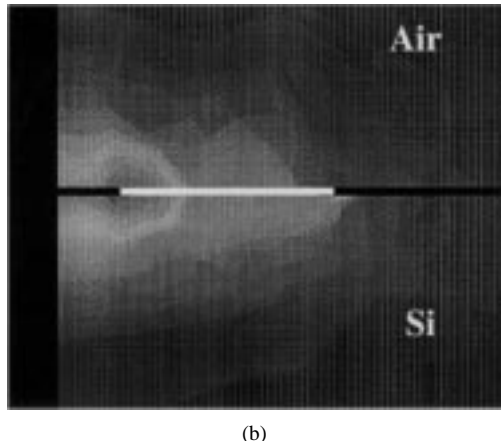


Fig. 4. ϵ_{eff} versus frequency for a 80–40–80- μm micromachined FGC with 4- and 12- μm undercut. Comparison with conventional FGC and 80–40–80- μm microshield.



(a)



(b)

Fig. 5. Field distribution. (a) Etched FGC. (b) Regular FGC.

the field concentrates in the air region where the material is etched away, resulting in a much lower effective dielectric constant, higher line impedance, and reduced ohmic loss. Loss reduction is evident from the measured data, shown in Fig. 6, where loss in decibels/millimeters is plotted versus frequency for $W-S-W$ lines of 45–20–45 μm for both conventional FGC and micromachined FGC with 4- μm undercut. The loss in the micromachined line is approximately 40% less

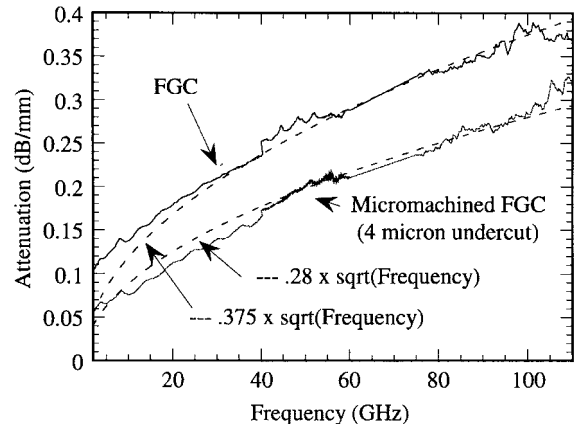


Fig. 6. Attenuation versus frequency for FGC line with 20- μm center conductor and 45- μm apertures compared with micromachined line of same geometry.

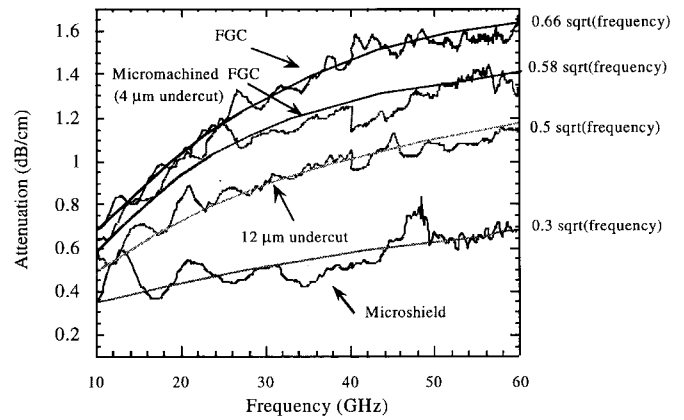


Fig. 7. Attenuation versus frequency. All lines have $W = 80 \mu\text{m}$, $S = 40 \mu\text{m}$. The micromachined lines have 4- and 12- μm undercut and the microshield line has a 75- Ω characteristic impedance.

than that of FGC approaching 0.25 dB/mm at 94 GHz. The loss in decibels/millimeters exhibits a square-root frequency dependence indicating dominance of conductor loss. Note, this is in contrast to conventional microstrip and CPW where dielectric in addition to radiation loss can increase the value of α to as high as 0.6–1 dB/mm, depending on the substrate thickness and dielectric constant.

Fig. 7 shows loss in decibels/millimeters for a 80–40–80- μm micromachined line measured from 10 to 60 GHz. The loss in this line has been reduced considerably to 0.115 dB/mm at 60 GHz. From the measured data, it is concluded that the loss is predominantly ohmic due to the observed square-root frequency dependence. The measured data of Fig. 7 are approximated by simple functions that vary proportionally to \sqrt{f} . Since this loss is only ohmic and has a known frequency dependence, we can expect a value of 0.15 dB/mm at 94 GHz. Similarly, Fig. 8 shows loss in decibels/centimeters for FGC and micromachined FGC lines with $W-S-W$ equal to 45–50–45 μm and indicates substantial reduction in loss with increasing undercut.

As previously discussed, both the conventional and micromachined finite-ground coplanar lines exhibit zero dispersion

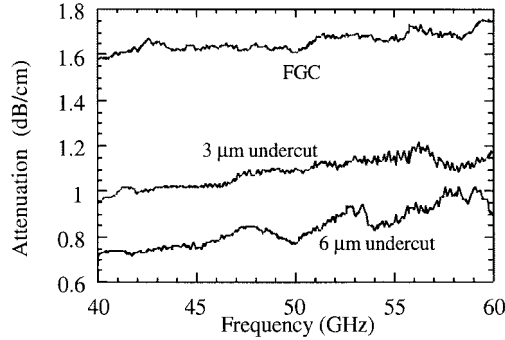


Fig. 8. Loss in decibels/centimeter in FGC and micromachined FGC lines with $S = 40$ and $W = 80 \mu\text{m}$.

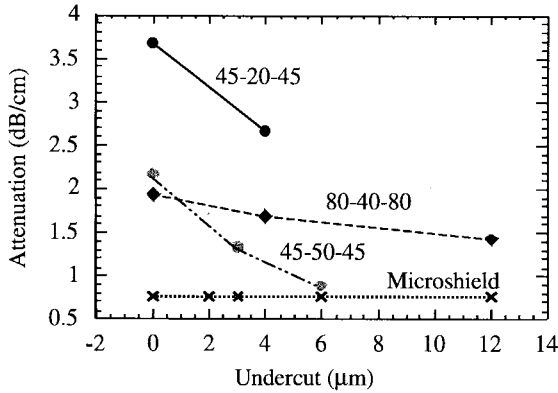


Fig. 9. Measured losses versus undercut at 94 GHz.

and only ohmic losses when designed according to the guidelines given in the previous sections. For micromachined FGC lines with the aspect ratios discussed herein, measurements up to W -band have confirmed the predominantly ohmic-loss behavior. Based on this, we could use the \sqrt{f} dependency to predict losses at 94 GHz for the lines studied herein. Fig. 9 shows ohmic loss in decibels/centimeters at 94 GHz for various lines as a function of undercut. Comparison of this loss to that of a 75Ω microshield line indicates the capability of the micromachined FGC to provide very competitive performance to that of membrane lines and rectangular waveguide, the loss of which approaches 0.025 dB/cm in W -band. Fig. 10 shows measured effective dielectric constant versus undercut for micromachined FGC lines with $W = 80 \mu\text{m}$ and $S = 40 \mu\text{m}$. The monotonic decrease of the effective dielectric constant with undercut indicates that the loss exhibited by the micromachined line in decibels/(guided wavelength) will not vary with the undercut as dramatically as it has been observed when the same loss is measured in decibels/centimeters. This implies that use of these lines is unquestionably beneficial in circuits where physical lengths remain fixed, such as antenna-feed networks. However, in circuits where electric lengths remain unchanged, micromachined lines will tend to provide less loss and reduced junction parasitics, but will result in longer circuit physical dimensions. In this case, the use of micromachined lines clearly depends on the tradeoff allowed by the circuits specifications and the objectives of the circuit designer.

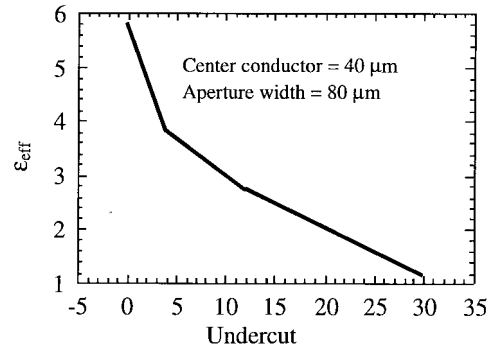


Fig. 10. Effective dielectric constant versus undercut for a micromachined FGC with $W-S-W$ equal to $80-40-80 \mu\text{m}$.

TABLE I
DECREASING ε_{eff} , DECREASING ATTENUATION (AT 94 GHz), AND
INCREASING CHARACTERISTIC IMPEDANCE FOR THREE DIFFERENT
ASPECT RATIO ($S/S + 2W$), WITH INCREASING UNDERCUT

Aspect ratio (S/W)	Parameters	Conventional FGC line (no undercut)	2 μm undercut	4 μm undercut	6 μm undercut	8 μm undercut	10 μm undercut
0.18 (20/45)	ε_{eff}	4.938	4.165	3.560	2.520	n/a	n/a
	α (dB/cm)	3.65	3.2	2.7	2.3	n/a	n/a
	Z_0 (Ω)	71	77.31	83.62	99.39	n/a	n/a
0.2 (40/80)	ε_{eff}	5.57	4.625	4.0	3.494	3.189	2.973
	α (dB/cm)	1.95	1.8	1.75	1.65	1.6	1.5
	Z_0 (Ω)	64	70.2	75.5	80.8	84.58	87.59
0.36 (50/45)	ε_{eff}	5.408	4.830	4.34	4.081	3.845	3.698
	α (dB/cm)	2.2	1.6	1.2	0.8	n/a	n/a
	Z_0 (Ω)	57	60.31	63.53	65.62	67.60	68.93

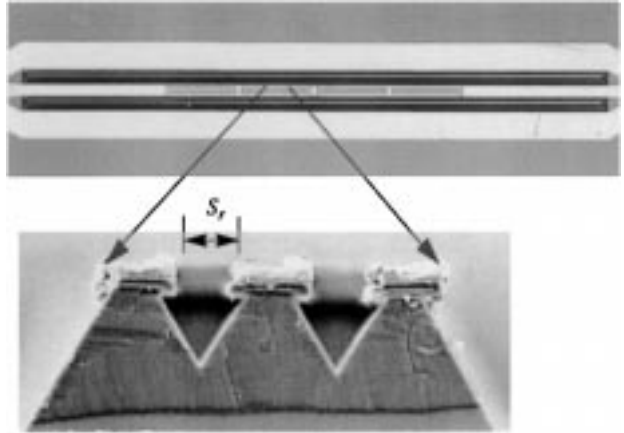


Fig. 11. Micromachined four-resonator bandpass filter with $w = 45 \mu\text{m}$ and $s = 50$ and $4 \mu\text{m}$ undercut.

From the measured micromachined FGC lines, design guidelines have been developed. Although there are different ways to present such data, tabular format has been used here, as seen in Table I, which shows the effect of removing material from the aperture regions with increasing lateral undercut, as compared to that of a conventional FGC line [32]. The general trend with increasing undercut is decreasing ε_{eff} , decreasing attenuation, and increasing characteristic impedance. These aspect ratios were chosen to ensure balanced single-mode

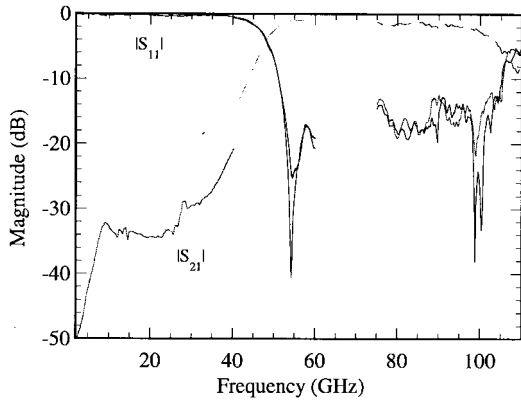


Fig. 12. Measured scattering parameters for the *V*-band filter of Fig. 11.

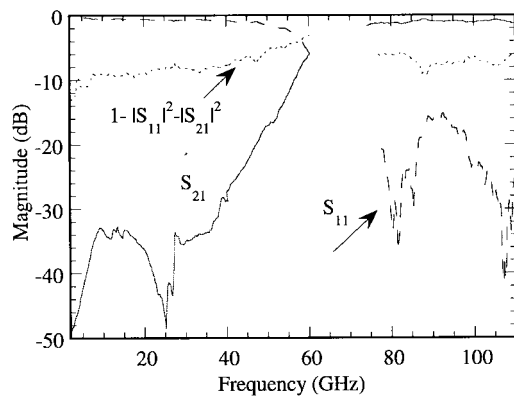


Fig. 13. Measured scattering parameters for the *W*-band filter of Fig. 11.

propagation, and lines with similar aspect ratios will behave accordingly.

IV. MICROMACHINED CPW *W*-BAND COMPONENTS

The micromachined FGC's described above have been used in the design of four-resonator *V*- and *W*-band bandpass filters, as shown in Fig. 11. The Si substrate has been etched away from the main lines (45–50–45 μm) and the resonator apertures ($S_r = 20 \mu\text{m}$) to allow for reduced loss and parasitics. The filters were etched for 2 h in EDP to introduce a 4- μm undercut.

Measured performance is shown in Figs. 12 and 13. The measured results for the *W*-band filter show a loss of 0.8 dB at 94 GHz, an improvement of 0.8 dB over a similar finite-ground coplanar filter with an insertion loss of 1.6 dB at the same frequency [25]. All the presented measurement results lack data points in the frequency range of 60–75 GHz due to lack of appropriate measurement equipment.

V. CONCLUSIONS

A new class of Si micromachined lines has demonstrated excellent performance, ease in design and fabrication, and very low cost in development. This is due to their ability to excite a TEM mode, operate free of parasitic parallel-plate modes, and operate without vias, resulting in single-side wafer processing. These lines have been extensively studied and have shown the potential to compete with membrane lines in terms of low-loss

performance. These lines have been used in the development of four-resonator *V*- and *W*-band filters, and have shown reduction in loss and improvement in the overall performance.

REFERENCES

- [1] N. I. Dib, W. P. Harokopus, L. P. B. Katehi, C. C. Ling, and G. M. Rebeiz, "A study of a novel planar transmission line," presented at the IEEE MTT-S Int. Symp., Boston, MA, June 1991.
- [2] D. F. Williams and S. E. Schwarz, "Reduction of propagation losses in coplanar waveguide," in *IEEE MTT-S Symp. Dig.*, San Francisco, CA, May 30–June 1, 1984, pp. 453–454.
- [3] T. M. Weller, G. M. Rebeiz, and L. P. B. Katehi, "Experimental results on microshield transmission line circuits," presented at the IEEE Int. MTT-S Symp., Atlanta, GA, June 1993.
- [4] T. M. Weller, L. P. B. Katehi, G. M. Rebeiz, H. J. Cheng, and J. F. Whitaker, "Fabrication and characterization of microshield circuits," presented at the Int. Symp. Space Terahertz Technol., Los Angeles, CA, Mar. 1993.
- [5] R. F. Drayton and L. P. B. Katehi, "Experimental study of micromachined circuits," in *Space Terahertz Technol. Int. Symp. Dig.*, Los Angeles, CA, Mar. 1993, pp. 238–248.
- [6] ———, "Microwave characterization of microshield lines," presented at the 40th ARFTG Conf. Dig., Orlando, FL, Dec. 1992.
- [7] ———, "Micromachined circuits for MM-wave applications," in *European Microwave Conf. Dig.*, Madrid, Spain, Sept. 1993, pp. 587–588.
- [8] H.-J. Cheng, J. F. Whitaker, T. M. Weller, and L. P. B. Katehi, "Terahertz-bandwidth characteristics of coplanar transmission lines on low permittivity substrates," *IEEE Trans. Microwave Theory Tech.*, vol. 42, pp. 2399–2406, Dec. 1994.
- [9] S. V. Robertson, L. P. B. Katehi, and G. M. Rebeiz, "Micromachined self-packaged *W*-band bandpass filters," in *IEEE MTT-S Symp. Dig.*, Orlando, FL, 1995, pp. 1543–1546.
- [10] T. Weller, L. Katehi, M. Herman, and P. Wamhof, "Membrane technology applied to microstrip: A 33 GHz Wilkinson power divider," in *IEEE MTT-S Symp. Dig.*, vol. 2, San Diego, CA, 1994, pp. 911–914.
- [11] R. F. Drayton, T. M. Weller, and L. P. Katehi, "Development of miniaturized circuits for high-frequency applications using micromachining techniques," *Int. J. Microcircuits Electron. Packaging*, vol. 18, no. 3, Third Quarter, 1995.
- [12] R. F. Drayton and L. P. B. Katehi, "Micromachined circuits for MM-wave applications," in *Proc. 23rd European Microwave Conf.*, Madrid, Spain, Sept. 1993, pp. 587–588.
- [13] ———, "Micromachined conformal packages for microwave and millimeter-wave applications," presented at the IEEE MTT-S Symp., Orlando, FL, May 1995.
- [14] L. P. B. Katehi *et al.*, "Si micromachining in high-frequency applications," *CRC Handbook on Si Micromachining*. Boca Raton, FL: CRC Press, 1995.
- [15] C. Goldsmith, T.-H. Lin, B. Powers, W.-R. Wu, and B. Norvell, "Micromechanical membrane switches for microwave applications," presented at the IEEE MTT-S Symp., Orlando, FL, May 1995.
- [16] M. I. Herman, K. A. Lee, E. A. Kolawa, L. E. Lowry, and A. N. Tulintseff, "Novel techniques for millimeter-wave packages," *IEEE Trans. Microwave Theory Tech.*, vol. 43, pp. 1516–1523, July 1995.
- [17] N. L. VandenBerg and L. P. B. Katehi, "Broad-band vertical interconnects using slot-coupled shielded microstrip lines," *IEEE Trans. Microwave Theory Tech.*, vol. 40, pp. 81–88, Jan. 1992.
- [18] L. P. B. Katehi, "Novel transmission lines for the submillimeter-wave region," *Proc. IEEE*, vol. 80, pp. 1771–1787, Nov. 1992.
- [19] R. F. Drayton, T. M. Weller, and L. P. Katehi, "Development of miniaturized circuits for high-frequency applications using micromachining techniques," *Int. J. Microcircuits Electron. Packaging*, vol. 18, no. 3, Third Quarter, 1995.
- [20] S. V. Robertson, L. P. B. Katehi, and G. M. Rebeiz, "Micromachined self-packaged *W*-band bandpass filters," in *IEEE MTT-S Symp. Dig.*, Orlando, FL, 1995, pp. 1543–1546.
- [21] L. P. B. Katehi, "Novel transmission lines for the submillimeter-wave region," *Proc. IEEE*, vol. 80, pp. 1771–1787, Nov. 1992.
- [22] K. Herrick, T. Schwartz, and L. P. B. Katehi, "W-band micromachined finite ground coplanar waveguide filters," in *IEEE MTT-S Symp. Dig.*, vol. 1, Denver, CO, June 1997, pp. 269–272.
- [23] G. Ponchak, M. Matloubian, and L. P. B. Katehi, "Losses in *W*-band finite ground coplanar waveguides," *Microwave Guided Wave Lett.*, to be published.
- [24] F. Brauchler, J. Papapolymerou, J. East, and L. P. B. Katehi, "W-band monolithic multipliers," in *IEEE MTT-S Symp. Dig.*, vol. 3, Denver, CO, June 1997, pp. 1225–1228.

- [25] F. Brauchler, S. Robertson, J. East, and L. Katehi, "W-band finite ground coplanar (FGC) line circuit elements," *IEEE Trans. Microwave Theory Tech.*, to be published.
- [26] F. Brauchler, J. East, and L. Katehi, "W-band FGC multipliers," *IEEE Trans. Microwave Theory Tech.*, to be published.
- [27] K.-C. Syao, K. Yang, X. Zhang, L.-H. Lu, L. P. B. Katehi, and P. Bhattacharya, "Investigation of adjacent channel crosstalk in multichannel monolithically integrated 1.55-mm photoreceiver arrays," *J. Lightweight Technol.*, vol. 15, Oct. 1997.
- [28] S. V. Robertson, M. Matloubian, M. Case, and L. P. B. Katehi, "A Si micromachined conformal package for a K-band low noise HEMT amplifier," in *IEEE MTT-S Symp. Dig.*, vol. 2, Denver, CO, June 1997, pp. 517-520.
- [29] R. M. Henderson and L. P. B. Katehi, "Silicon-based micromachined packages for discrete components," in *IEEE MTT-S Symp. Dig.*, vol. 2, Denver, CO, June 1997, pp. 521-524.
- [30] ———, "Si-based micromachined packages for high-frequency applications," *IEEE Trans. Microwave Theory Tech.*, to be published.
- [31] Z. R. Hu *et al.*, "Characteristics of trenched coplanar waveguide for SiMMIC applications," presented at the *Proc. IEEE MTT-S Symp.*, Denver, CO, June 1997.
- [32] L. P. B. Katehi, "Power cube first design meeting," *Quart. Rep. RL-956*, Radiation Lab., Univ. Michigan, Ann Arbor, Dec. 1996.



Katherine Juliet Herrick was born in Rochester, NY, on July 2, 1971. She received the B.S.E. and M.S.E. degrees in electrical engineering from the University of Michigan at Ann Arbor, in 1993 and 1995, respectively, and is currently working toward the M.S.E. degree in biomedical engineering and the Ph.D. degree in electrical engineering. Her research interests include microwave and millimeter-wave circuits, micromachining, packaging, and solid-state technology. She is currently working on compact vertical interconnects for multilayer MMIC applications.

Ms. Herrick is a member of Sigma Xi. She received the Best Student Paper Award at the 1997 IEEE International Microwave Symposium.

Thomas A. Schwarz was born in Cadillac, MI, on October 30, 1975. He is working toward the B.S.E. degree in electrical engineering at the University of Michigan at Ann Arbor.

He is currently an Undergraduate Research Assistant, with interests in numerical modeling and fabrication of microwave circuits.



Linda P. B. Katehi (S'81-M'84-SM'89-F'95) received the B.S.E.E. degree from the National Technical University of Athens, Athens, Greece, in 1977, and the M.S.E.E. and Ph.D. degrees from the University of California at Los Angeles, in 1981 and 1984, respectively.

In September 1984, she joined the faculty of the EECS Department, University of Michigan at Ann Arbor. Since then, she has been interested in the development and characterization (theoretical and experimental) of microwave, millimeter printed circuits, the computer-aided design of VLSI interconnects, the development and characterization of micromachined circuits for millimeter-wave and submillimeter-wave applications, and the development of low-loss lines for terahertz-frequency applications. She has also been theoretically and experimentally studying various types of uniplanar radiating structures for hybrid-monolithic and monolithic oscillator and mixer designs.

Dr. Katehi is a member of IEEE Antennas and Propagation and Microwave Theory and Techniques Societies, Sigma Xi, Hybrid Microelectronics, URSI Commission D and a member of AP-S ADCOM (1992-1995). She is an associate editor for the *IEEE TRANSACTIONS ON MICROWAVE THEORY AND TECHNIQUES*. She was awarded the IEEE AP-S R. W. P. King Best Paper Award for a Young Engineer in 1984, the IEEE AP-S S. A. Schelkunoff Best Paper Award in 1985, the NSF Presidential Young Investigator Award and URSI Young Scientist Fellowship in 1987, the Humboldt Research Award and The University of Michigan Faculty Recognition Award in 1994, the IEEE MTT-S Microwave Prize in 1996, and the International Microelectronics and Packaging Society (IMAPS) Best Paper Award in 1997.